

# Microtubes and nanotubes of a phospholipid bilayer membrane

Veronika Kralj-Iglič<sup>1</sup>, Aleš Iglič<sup>2</sup>, Gregor Gomišček<sup>1</sup>, France Sevšek<sup>1</sup>,  
Vesna Arrigler<sup>1</sup> and Henry Hägerstrand<sup>3</sup>

<sup>1</sup> Institute of Biophysics, Faculty of Medicine, Lipičeva 2, SI-1000 Ljubljana, Slovenia

<sup>2</sup> Laboratory of Applied Physics, Faculty of Electrical Engineering, Tržaška 2, SI-1000 Ljubljana, Slovenia

<sup>3</sup> Department of Biology, Åbo Akademi University, Biocity, FIN-20520 Åbo/Turku, Finland

Received 28 September 2001, in final form 17 December 2001

Published 8 February 2002

Online at [stacks.iop.org/JPhysA/35/1533](http://stacks.iop.org/JPhysA/35/1533)

## Abstract

We propose a theory describing the stable structure of a phospholipid bilayer in pure water involving a spherical mother vesicle with long thin tubular protrusion. It is considered that the phospholipid molecules are in general anisotropic with respect to the axis normal to the membrane and can orient in the plane of the membrane if the curvature field is strongly anisotropic. Taking this into account, the membrane free energy is derived starting from a single-molecule energy and using methods of statistical mechanics. By linking the description on the microscopic level with the continuum theory of elasticity we recover the expression for the membrane bending energy and obtain an additional (deviatoric) contribution due to the orientational ordering of the phospholipid molecules. It is shown that the deviatoric contribution may considerably decrease the phospholipid vesicle membrane free energy if the vesicle involves regions where the difference between the two principal curvatures is large (thin cylindrical protrusions and/or thin finite necks) and thereby yields a possible explanation for the stability of the long thin tubular protrusions of the phospholipid bilayer vesicles. We report on the experiment exhibiting a stable shape of the spherical phospholipid vesicle with a long thin tubular protrusion in pure water.

PACS numbers: 81.07.De, –5.70.–a, 82.70.Uv, 87.16.Dg

## 1. Introduction

Nano and microtubular structures have recently become a subject of increasing interest due to their importance in technology. Carbon nanotubes [1] are being extensively studied [2]. However, nanotubes composed of other materials such as boron nitride [3], metal dichalcogenides [4], TiO<sub>2</sub> [5], GaN [6], Sb<sub>2</sub>O<sub>3</sub> and Sb<sub>2</sub>O<sub>5</sub> [7] and NbS<sub>2</sub> [8] have also

been synthesized and explored. Besides in inorganic systems, long thin structures have also been found in organic systems such as in surfactant systems [9–11], in phospholipid systems [9, 12, 13], in erythrocytes in suspension under special conditions [14–16], and in cells [17, 18]. It was suggested [12] that the long thin tubular membranous structures may have an important role in living systems. It is only that they have long been overlooked due to their thinness and fragility that prevented their preservation for observation.

The almost flat bilayer structures of amphiphilic molecules have been thoroughly investigated in the last thirty years and are theoretically well explored (for a review see [19]). In contrast, studies involving micro- and nanotubes of amphiphilic molecules are not so numerous and the essential features involved in these systems could still be further clarified.

Stable tubes can be explained on the basis of the tilt of the membrane constituents and chirality [20–22]. It was shown [22] that the stable tubular shape corresponds to the minimum of the membrane free energy obtained by expansion over the curvature and nematic fields. For a nonzero chirality parameter, stable tubes were obtained with uniform orientational ordering and also with a periodic helical variation in orientational ordering within stripe-like domains. Further, the proposed theory describes modulation of the degree of twist of the ribbons formed by dimeric surfactants associated with chiral counterions [11]. Stable tubes were also obtained by considering a difference in the tilt within the two membrane layers composed of nonchiral molecules [23], by considering crystallization of anisotropic membrane constituents [24] and by para-antimematic ordering of the phospholipid molecules [25].

On the other hand, in studying bilayer structures decorated with inclusions, it was suggested [26] that stable tubular structures can be explained by considering deviatoric membrane elasticity that is a consequence of quadrupolar ordering of anisotropic membrane inclusions within the plane of the membrane. Further elaboration of this mechanism yielded a condition regarding the effective shape of the inclusions that induce spherical/tubular nanoexovesicles to be released from the erythrocyte membrane upon addition of different surfactants to the erythrocyte suspension [15]. Thereby it was explained why the dimeric surfactants yield tubular nanoexovesicles [15]. Further, stability of tubular tethers connecting the mother cell and the daughter vesicle in the extreme pH in the outer solution of the erythrocytes could be theoretically described by the quadrupolar ordering of the anisotropic membrane inclusions [16].

Recently, stable thin tubular structures have been observed as attached to giant palmitoyloleoylphosphatidylcholine (POPC) bilayer vesicles that were formed in an alternating electric field in sugar solution [13]. It was reported [13] that immediately after being placed into the observation chamber the vesicles are spherical; the protrusions are not visible under the phase contrast microscope and the long wavelength fluctuations of the spherical part are not observed. After some time, long thin protrusions become visible; the protrusions appear as very long thin tubes that are connected to the mother vesicle at one end while the other end is free. With time, the protrusion becomes shorter and thicker, however, the tubular character of the protrusion is still preserved; the fluctuations of the mother vesicle increase in strength. Later, undulations of the protrusion appear and become increasingly exhibited. Shortened protrusions may look like beads connected by thin necks. Eventually, the protrusion is completely integrated into the vesicle membrane to yield a fluctuating globular vesicle. However, the transformation of the protrusion is usually very slow, indicating that all the observed shapes may be considered as quasiequilibrium shapes. In the sample, the tubular protrusions are still observed several hours after the formation of the vesicles.

It was suggested [13] that the observed shape transformation is driven by the inequality of the chemical potential of the phospholipid molecules in the outer solution and in the outer membrane layer which causes a decrease in the difference between the outer and the inner

membrane layer areas. The possible mechanisms that were suggested to contribute to this are the drag of the lipid from the outer solution by the glass walls of the chamber, chemical modification of the lipid and phospholipid flip-flop [13]. A decrease of the volume to area ratio of the vesicle occurs due to slight evaporation of water from the chamber. The vesicle then loses water in order to equalize the respective chemical potentials inside and outside the vesicle.

The tubular/beadlike character of the protrusion seems to depend on the speed of the loss of the lipid molecules from the outer membrane layer relative to the speed of the decrease of the enclosed volume. The undulations of the protrusion are more noticeable when a small void is left in the grease thereby enhancing the evaporation of water from the outer solution. The complete picture of the dynamics of the shape transformation seems at this point beyond our understanding. However, we can point to some facts that can be stated with certain confidence: comparing the protrusions at an early time with a later time, the protrusions at the early time appear considerably more tubular. Therefore, we think that the protrusions have a tubular character also even at earlier times when they are too thin to be seen by the phase contrast microscope. Such thin tubular protrusions that may stay invisible for hours and are therefore considered to be (quasi) stable are the scope of this study.

It is our aim to investigate the possible mechanisms responsible for the stability of the tubular shapes. In particular, we study the case when the tubular protrusion is attached to the spherical mother vesicle. We generalize the description of the membrane inclusions [15, 16, 26] by considering the effect of all the phospholipid molecules that constitute the membrane. We derive the membrane free energy from a single-constituent energy and show that quadrupolar orientational ordering of the constituent molecules in a strong curvature field may explain stable thin tubular protrusions attached to the spherical vesicles. We performed an experiment similar to the one reported in [13] by using nonchiral constituents in pure water. The temperature was well above the temperature of the gel to liquid crystal phase transition of POPC (below 5 °C) [27], so that it is unlikely that the phospholipid molecules were tilted. We report that stable tubular structures were found also in such system, in agreement with theoretical results.

## 2. Theory

### 2.1. Statistical mechanical derivation of the free energy of a phospholipid bilayer

The shape of the mother vesicle and the protrusion fluctuate, therefore when we describe the shape, we mean some equilibrium shape that corresponds to a local minimum subject to these fluctuations. In order to describe the equilibrium shape with a long thin tubular protrusion we propose that specific molecular structure and local interactions of the phospholipid molecules should be considered in deriving the membrane free energy. In particular, it is taken into account that the phospholipid molecule, composed of the head and two tails, is in general anisotropic with respect to the director vector pointing in the direction of the membrane normal. It is assumed that in a highly anisotropic curvature field all orientations with respect to the director are not energetically equivalent, and that the molecule may spend on average more time in some preferred orientation.

To introduce the interaction of a chosen phospholipid molecule with the surrounding molecules, the chosen molecule is treated as an inclusion in a mean curvature field [29]. The derivation of the contribution of the inclusions to the membrane free energy is described in a previous paper [29]. In our case, where we have only one kind of molecule constituting the membrane, the mean curvature field at the site of the chosen phospholipid molecule is created

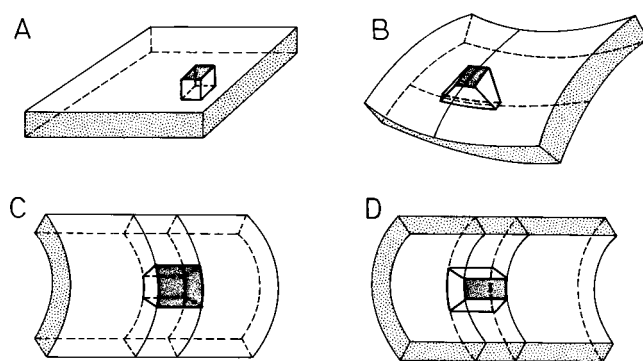


**Figure 1.** Schematic presentation of four different intrinsic shapes: (A) flat shape ( $H_m = 0$ ,  $D_m = 0$ ), (B) saddle shape ( $H_m \neq 0$ ,  $D_m \neq 0$ ), (C) cylinder ( $H_m > 0$ ,  $|D_m| = H_m$ ), (D) inverted cylinder ( $H_m < 0$ ,  $|D_m| = -H_m$ ).

by the phospholipid molecules that surround the chosen molecule. To describe the interaction between the chosen molecule and the local curvature field we use the basic assumptions presented in [29]: it is assumed that there exists a membrane shape that would completely fit the inclusion, i.e. no energy would be required to insert the inclusion into such a membrane. We call it the shape intrinsic to the inclusion, or the intrinsic shape. The corresponding main curvatures are referred to as the intrinsic main curvatures and denoted by  $C_{1m}$  and  $C_{2m}$ . In the following we also use the parameter intrinsic mean curvature  $H_m = \frac{1}{2}(C_{1m} + C_{2m})$  and the parameter  $D_m = \frac{1}{2}(C_{1m} - C_{2m})$ . Figure 1 gives a schematical presentation of four different intrinsic shapes: (A) flat shape ( $H_m = 0$ ,  $D_m = 0$ ), (B) saddle shape ( $H_m \neq 0$ ,  $D_m \neq 0$ ), (C) cylinder ( $H_m > 0$ ,  $|D_m| = H_m$ ), (D) inverted cylinder ( $H_m < 0$ ,  $|D_m| = -H_m$ ). If the membrane had the intrinsic shape over all its area, the energy of such a shape would be zero. However, if we consider a closed shape subject to geometrical constraints, the membrane cannot have such curvature in all its points. The shape of the membrane at a chosen point is given by the two principal curvatures  $C_1$  and  $C_2$ , the corresponding mean curvature  $H = \frac{1}{2}(C_1 + C_2)$  and the parameter  $D = \frac{1}{2}(C_1 - C_2)$ . The single-molecule energy is defined as the energy of the mismatch between the local curvature and the intrinsic curvature [29],

$$E(\omega) = \frac{\xi}{2}(H - H_m)^2 + \frac{1}{2} \frac{\xi + \xi^*}{2} (D^2 - 2DD_m \cos(2\omega) + D_m^2) \quad (1)$$

where  $\xi$  and  $\xi^*$  are the interaction constants and  $\omega$  is the orientation of the principal system of the molecule with respect to the principal system of the membrane continuum. As the phospholipid molecule is considered to be anisotropic,  $D_m \neq 0$ .

To account for different orientational states of the molecule, the single-molecule partition function is introduced [26],

$$q_i = \frac{1}{\omega_0} \int_0^{2\pi} \exp\left(-\frac{E(\omega)}{kT}\right) d\omega \quad (2)$$

where  $\omega_0$  is an angle quantum,  $k$  is the Boltzmann constant and  $T$  is the temperature. The free energy of the single molecule is then obtained by

$$F_i = -kT \ln q_i. \quad (3)$$

The contribution to the membrane free energy due to local interaction between the molecules and the mean curvature field is in the first approximation obtained by summing the contributions of the individual molecules of both layers,

$$F = \int n_{\text{out}} F_i(C_1, C_2) dA + \int n_{\text{in}} F_i(-C_1, -C_2) dA \quad (4)$$

where  $n_{\text{out}}$  and  $n_{\text{in}}$  are the area densities of the molecules in the outer and the inner membrane layers, respectively. The integration is performed over the membrane area  $A$ . Note that the principal curvatures in the inner layer have signs opposite to the signs of the principal curvatures of the outer layer due to the specific configuration of the phospholipid molecules within the layers—touching tails.

If we assume for simplicity that the area densities are constant over the respective layers and also equal,  $n_{\text{out}} = n_{\text{in}} = n_0$ , and insert the expression for the single-molecule energy (equation (1)) into equation (4), we obtain

$$F = n_0 \xi \int H^2 dA + n_0 \frac{\xi + \xi^*}{2} \int D^2 dA - 2n_0 kT \int \ln \left( I_0 \left( \frac{\xi + \xi^*}{2kT} DD_m \right) \right) dA \quad (5)$$

where  $I_0$  is the modified Bessel function [26, 29]. In integrating, the differences in the areas of the inner and the outer layers are disregarded, so that the contributions proportional to the intrinsic mean curvature  $H_m$  of the inner and the outer layers cancel and there is no spontaneous curvature for the bilayer vesicles composed of a single species of molecules. Also, in equation (5), the constant terms are omitted.

The first and second terms of equation (5) can be combined by using the equation

$$H^2 = D^2 + C_1 C_2 \quad (6)$$

to yield

$$F = W_b + F_d \quad (7)$$

where

$$W_b = n_0 \frac{3\xi + \xi^*}{8} \int (2H)^2 dA - n_0 \frac{\xi + \xi^*}{2} \int C_1 C_2 dA \quad (8)$$

and

$$F_d = -2kT n_0 \int \ln \left( I_0 \left( \frac{\xi + \xi^*}{2kT} DD_m \right) \right) dA. \quad (9)$$

## 2.2. Thermodynamic link

The obtained expressions (7)–(9) are compared to the bending energy of the almost flat thin membrane [30] with zero spontaneous curvature

$$W_b = \frac{k_c}{2} \int (2H)^2 dA + k_G \int C_1 C_2 dA \quad (10)$$

where  $k_c$  and  $k_G$  are the membrane local and Gaussian bending constants, respectively. We can see that the statistical mechanical derivation recovers the expression (10), where  $n_0(3\xi + \xi^*)/4 = k_c$  and  $-n_0(\xi + \xi^*)/2 = k_G$ , and also yields an additional contribution (equation (9)) due to the orientational ordering of the phospholipid molecules. This contribution, which is always negative, is called the deviatoric elastic energy of the membrane (originating in the curvature deviator  $|D|$ ). It can also be seen that the constant before the Gaussian curvature in equation (8) is negative.

Introducing the dimensionless quantities, the energy  $F$  (equation (7)) and its terms (equations (8) and (9)) are normalized by  $2\pi n_0(3\xi + \xi^*)$ ,

$$f = w_b + f_d \quad (11)$$

$$w_b = \frac{1}{4} \int (2h)^2 da + \kappa_G \int c_1 c_2 da \quad (12)$$

$$f_d = -\kappa \int \ln(I_0(\vartheta d_m d)) da \quad (13)$$

where  $da = dA/4\pi R^2$ ,

$$R = (A/4\pi)^{1/2} \quad (14)$$

$$\kappa_G = -(\xi + \xi^*)/(3\xi + \xi^*) \quad (15)$$

$$\kappa = 4kTR^2/(3\xi + \xi^*) \quad (16)$$

$$\vartheta = (\xi + \xi^*)/2kTR^2 \quad (17)$$

$c_1 = RC_1$ ,  $c_2 = RC_2$ ,  $h = RH$ ,  $d = RD$  and  $d_m = RD_m$ .

We obtain the dimensionless bending energy (equation (12)) if we normalize the expression (10) by  $8\pi k_c$ . Thereby,

$$\kappa_G = k_G/2k_c. \quad (18)$$

To estimate the interaction constants, we assume that the conformation of the phospholipid molecules is equal all over the membrane and take for simplicity that  $\xi = \xi^*$ . In this case,  $\kappa_G = -1/2$ . It follows then from equation (18) that  $k_G = -k_c$ . By comparing the constants before the first terms of equations (9) and (10) we can express the interaction constant  $\xi$  by the measured quantities: the local bending constant  $k_c$  and the area density of the number of phospholipid molecules  $n_0$ , so that

$$\xi = k_c/n_0 \quad (19)$$

and

$$\kappa = 1/\vartheta = kTR^2 n_0/k_c. \quad (20)$$

We consider that  $k_c \simeq 20kT$  [31, 32] and that  $n_0 = 1/a_0$  where  $a_0$  is the area per molecule,  $a_0 \simeq 0.6 \text{ nm}^2$  [33],  $T = 300 \text{ K}$  and  $R = 10^{-5} \text{ m}$ . This gives  $\kappa = 1/\vartheta \simeq 8.3 \times 10^6$ . We estimate that the upper bound of  $D_m$  is the inverse of the molecular dimension ( $\simeq 10^8 \text{ m}^{-1}$ ) so that in our case  $d_m = RD_m$  would be of the order  $10^3$ .

### 2.3. Determination of the equilibrium shape of the phospholipid vesicle with a long thin protrusion

The equilibrium shape is determined by the minimum of the membrane free energy (equations (7)–(9)) at given constraints. It is taken that the membrane area  $A$  and the enclosed volume  $V$  are fixed. Also, the bilayer couple principle [34] is applied [35] by the constraint requiring a fixed difference between the two membrane layer areas

$$\Delta A = \delta \int (2H) dA \quad (21)$$

where  $\delta$  is the distance between the two layer neutral areas which is considered to be small with respect to  $1/H$ . The quantity  $\Delta A$  is assumed to reflect the conditions in which the

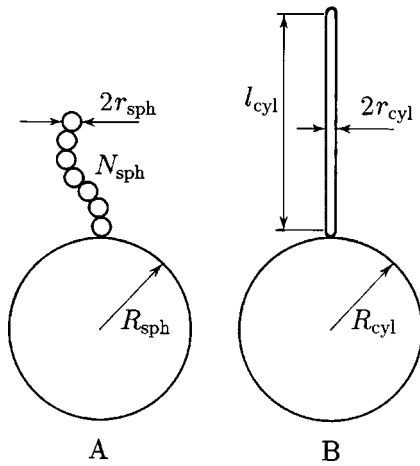


**Figure 2.** Schematic presentation of the shape composed of the mother sphere and the protrusion composed of small spheres connected by infinitesimal necks (A) and of the shape composed of the mother sphere and a thin cylinder closed by hemispherical caps (B).

vesicle formation took place and is determined by the number of phospholipid molecules that constitute the respective layers.

The membrane area, the enclosed volume and the area difference (equation (21)) are also given in dimensionless form. According to the choice of unit length  $R$  (equation (14)), the dimensionless membrane area is  $a = 1$ , the dimensionless volume (i.e. the relative volume) is  $v = (36\pi V^2/A^3)^{1/2}$ , while the area difference  $\Delta A$  is normalized by  $8\pi\delta R$  to yield the dimensionless form  $\Delta a = \int h da$ .

The equilibrium shape of the phospholipid vesicle is determined by the minimum of the membrane free energy at constant membrane area and constant enclosed volume. Due to simplicity, in this study we will compare two shapes that represent the limits of the class of shapes with a long thin protrusion. In the first case the protrusion consists of equal small spheres (figure 2(A)) while in the second case the protrusion consists of a cylinder closed by hemispherical caps (figure 2(B)). It is expected that these two limit shapes are continuously connected by a sequence of shapes with decreasingly exhibited undulations of the protrusion. As in this paper we focus on the general behaviour of the system, we do not consider the intermediate shapes explicitly.

Each of these two limit cases involves three geometrical model parameters (figure 2). In the shape with small spheres these parameters are the radius of the spherical mother vesicle  $R_{\text{sph}}$ , the radius of the small spheres  $r_{\text{sph}}$  and the number of small spheres  $N$  (figure 2(A)). As in long thin protrusions  $N$  is expected to be large, any real number is allowed for the parameter  $N$ . In the shape with the cylinder these parameters are the radius of the spherical mother vesicle  $R_{\text{cyl}}$ , the radius of the cylinder and the closing hemispheres  $r_{\text{cyl}}$ , and the length of the cylinder  $l$  (figure 2(B)).

From geometrical constraints for the relative area  $a = 1$ , the relative volume  $v$  and the relative area difference  $\Delta a$ , the three parameters that determine the shape in both cases (the radius of the mother sphere, the radius of small spheres/cylinder and the number of small spheres/length of the cylinder) are derived.

It is taken that the relative volume is close to 1. For the shape with small spheres, the radius of the mother sphere  $R_{\text{sph}}$  is taken to be  $R_{\text{sph}} \simeq 1 - x$ , where  $x$  is small. Keeping the terms of the first order yields

$$R_{\text{sph}} = \frac{2 + v}{3} \quad (22)$$

$$r_{\text{sph}} = \frac{2(1-v)}{3(\Delta a - \frac{2+v}{3})} \quad (23)$$

$$N = \frac{3(\Delta a - \frac{2+v}{3})^2}{2(1-v)}. \quad (24)$$

For the shape with the cylinder,  $R_{\text{cyl}} \simeq 1 - x$  and the respective quantities are

$$R_{\text{cyl}} = \frac{2+v}{3} \quad (25)$$

$$r_{\text{cyl}} = \frac{(1-v)}{3(\Delta a - \frac{2+v}{3})} \quad (26)$$

$$l = 4 \left( \Delta a - \frac{2+v}{3} \right). \quad (27)$$

Within the above approximation ( $v \simeq 1$ ) the relative radius of the mother vesicle is equal to  $(2+v)/3$  in both cases (equations (22) and (25)) and the area differences of the protrusions of both shapes are equal.

The relative free energy of the membrane is calculated by applying equations (11)–(13) to the respective geometries.

If the deviatoric term were not taken into account the shape with the beadlike protrusion would yield

$$w_{\text{b,sph}} = 1 + N + \kappa_G \quad (28)$$

while the shape with the cylindrical protrusion would yield

$$w_{\text{b,cyl}} = 2 + \frac{l}{8r_{\text{cyl}}} + \kappa_G. \quad (29)$$

As the topology of both shapes is the same, the respective Gaussian terms are equal. By inserting for  $N$  equation (24) and for  $l$  and  $r_{\text{cyl}}$  equations (27) and (26), respectively, we can see that

$$w_{\text{b,cyl}} = w_{\text{b,sph}} + 1. \quad (30)$$

It follows from equation (30) that within the elasticity theory of the isotropic bilayer membrane, the shape with the protrusion composed of small spheres that are connected with infinitesimal necks would always be favoured over the shape with the tubular protrusion. Therefore, this theory is unable to explain stable tubular protrusions.

In considering the deviatoric effect, we assume that there is no deviatoric contribution in the shape composed of spheres connected by infinitesimal necks. At spherical parts there is no deviatoric contribution as the local deviator is equal to zero (see equation (13)). In the infinitesimal neck, the curvature deviator is very large, whereas the area of the neck is very small. Numerical calculations of the membrane free energy of the shape sequence leading to two spheres connected by the infinitesimal neck have shown that as the limit shape is approached, the deviatoric contribution of the neck diminishes [29]. Therefore, for the shape composed of spheres connected by infinitesimal necks the free energy is expressed by equation (28).

In the shape with the cylindrical protrusion we consider the deviatoric contribution of the cylindrical part. Also here, we consider that there is no deviatoric contribution of the



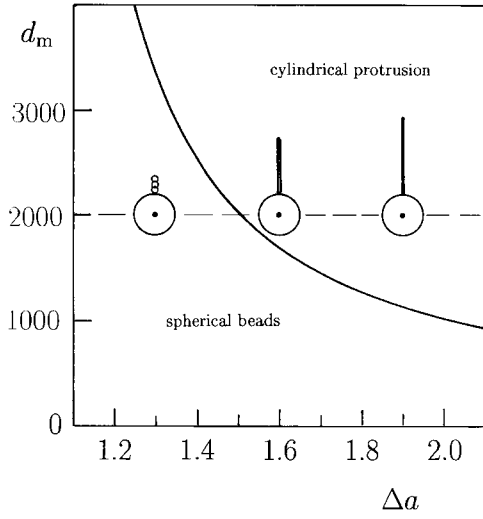


**Figure 3.** A  $(d_m, \Delta a)$  phase diagram of calculated equilibrium shapes with protrusions. The regions where the shapes with the respective kind of protrusions are energetically more favourable are indicated. The sequence of shapes shown in the figure indicates the process of diminishing  $\Delta a$  at constant  $v$  that could be observed in experiments. It was chosen that  $a_0 = 0.6 \text{ nm}^2$ ,  $R = 10^{-5} \text{ m}$ ,  $k_c = 20kT$ , so that  $\kappa = 1/\vartheta = 8.3 \times 10^6$  while  $v = 0.95$ . The shapes corresponding to different  $\Delta a$  are depicted with the centre of the spherical part at the respective  $\Delta a$  values.

neck connecting the mother sphere and the protrusion. As the relative deviator  $d = 1/2r_{\text{cyl}}$  is constant over the area of the cylindrical part  $r_{\text{cyl}}l/2$ , we obtain by using equation (13)

$$f_{d,\text{cyl}} = -\frac{2}{3}\kappa(1-v) \ln \left( I_0 \left( \frac{\vartheta d_m 3 \left( \Delta a - \frac{2+v}{3} \right)}{2(1-v)} \right) \right). \quad (31)$$

The topology of both shapes (*A* and *B*, figure 2) is the same, therefore the respective Gaussian terms are equal.

By choosing the parameters  $v$  and  $\Delta a$ , the geometrical parameters for both shapes (figures 2(A) and (B)) are determined (equations (22)–(24) and (25)–(27), respectively), and the energies for both shapes are calculated. By comparing the values of the free energies we can see which shape yields the lowest membrane free energy at the chosen  $v$  and  $\Delta a$ . If we choose high  $\Delta a$  the shape has a long protrusion. As the membrane area and the enclosed volume are fixed, this protrusion is very thin and consequently its mean curvature is large. For the tubular protrusions the deviatoric contribution is large enough to compensate for the less favourable bending energy of the cylinder. On the other hand, for lower  $\Delta a$ , the protrusion of the same membrane area and enclosed volume is shorter and broader, therefore its mean curvature is lower. The corresponding deviatoric term of the cylinder is too small to be of importance and the shape with the beadlike protrusion has lower free energy. At a chosen intrinsic anisotropy  $d_m$ , the shapes with small spheres are energetically more favourable below a certain  $\Delta a$  while above this threshold the shapes with cylinders are favoured.

Figure 3 shows the  $(d_m, \Delta a)$  phase diagram exhibiting the regions corresponding to the calculated stable shapes composed of the spherical mother vesicle and tubular protrusion and to the stable shapes composed of the spherical mother vesicle and the protrusion consisting of small spheres connected by infinitesimal necks.

The calculated geometrical parameters and energy contributions for the three shapes depicted in figure 3 are given in table 1. The deviatoric contribution of the shape with the cylinder is also given in  $kT$  units. It can be seen that the radii of the stable tubular protrusion are in the range of  $10^{-7} \text{ m}$  and that the corresponding deviatoric energies are larger than the estimated energy of thermal fluctuations. It can also be seen from table 1 that for this particular choice of the parameters the dimensionless radius of the stable cylindrical protrusions is about 0.02–0.04, which means that the corresponding cylinder radius would be about 200–400 nm.

**Table 1.** The geometrical parameters and the energies of the shapes depicted in figure 2.  $\Delta a$ : the normalized difference between the two membrane layer areas,  $r_{\text{sph}}$ : the normalized radius of the small spheres,  $N$ : the number of small spheres,  $f_{\text{sph}}$ : the normalized free energy of the shape with spherical beads,  $l_{\text{cyl}}$ : the normalized length of the cylindrical part of the protrusion,  $f_{\text{cyl}}$ : the normalized free energy of the shape with the cylindrical protrusion,  $f_{\text{dev}}$ : the normalized deviatoric contribution to the membrane free energy of the cylindrical protrusion,  $F_{\text{dev}}/kT$ : the deviatoric contribution to the membrane free energy in  $kT$  units. The data used in the calculation are  $k_c = 20kT$ ,  $a_0 = 0.6 \text{ nm}^2$ ,  $R = 10^{-5} \text{ m}$ ,  $v = 0.95$ ,  $d_m = 2000$ , which give  $\kappa = 1/\vartheta = 8.3 \times 10^6$  and  $R_{\text{sph}} = R_{\text{cyl}} = 0.98$ .

$\Delta a$	$r_{\text{sph}}$	$N$	$f_{\text{sph}}$	$r_{\text{cyl}}$	$l_{\text{cyl}}$	$f_{\text{cyl}}$	$f_{\text{dev}}$	$F_{\text{dev}}/kT$
1.3	0.100	3.0	4.0	0.050	1.27	4.65	-0.36	-181
1.6	0.054	11.41	12.41	0.027	2.47	12.04	-1.37	-688
1.9	0.036	25.21	26.21	0.018	3.67	24.18	-3.02	-1520

The sequence of shapes shown in the figure roughly simulates the transformation observed in the experiment [13]. Initially,  $\Delta a$  is large and the shape is composed of a mother sphere and a long thin nanotube. Assuming that the volume of the vesicle remains constant, with time, the number of phospholipid molecules in the outer layer diminishes, therefore  $\Delta a$  decreases and the tubular protrusion becomes thicker and shorter. In the experiment [13], the undulations of the protrusion become increasingly noticeable along the process. Our theoretical results shown in figure 3 exhibit a discontinuous transition from the tubular protrusion to the protrusion composed of small spheres connected by infinitesimal necks as we consider only the limits of the given class of shapes. Therefore, the phase diagram and the sequence (figure 3) should be viewed only as an indication of the tendency of the shape transition and not of the details of the shape.

### 3. Experiment

The phospholipid 1-palmitoyl-2-oleoyl-sn-glycero-3-phosphocholine (POPC) was purchased from Avanti Polar Lipids. The vesicles were made by the modified method of electroformation [28]. The experiment was performed at room temperature.

In the procedure, 20  $\mu\text{l}$  of phospholipid dissolved in 2:1 chloroform/methanol mixture, was spread over a pair of platinum electrodes. The solvent was allowed to evaporate for 2 h. The electroformation chamber with platinum electrodes was then filled with 2 ml of water. An alternating electric field was applied as described in [13]. The contents of the chamber were poured out into a plastic beaker. Then the chamber was filled with 2 ml water and the contents of the chamber were added to the solution that was already in the plastic beaker. The solution was gently mixed.

Immediately after the preparation, the solution containing the vesicles was placed into the observation chamber made by a pair of cover glasses and sealed by grease. The vesicles were observed by the inverted microscope Zeiss IM 35 with phase contrast optics.

In preparing the vesicles we used the same procedure as reported in [13], only that in the procedure presented in this paper we added no sugar to the solution in which the vesicles were formed, nor to the solution with which the vesicles were rinsed into the observation chamber. Previously [13] we added sucrose to the solution in which the vesicles were formed and glucose to the solution with which the vesicles were rinsed into the observation chamber. We used iso-osmolar solutions, therefore the vesicles containing the heavier sugar (sucrose) sank to the bottom of the observation chamber and made the observation easier. In the present

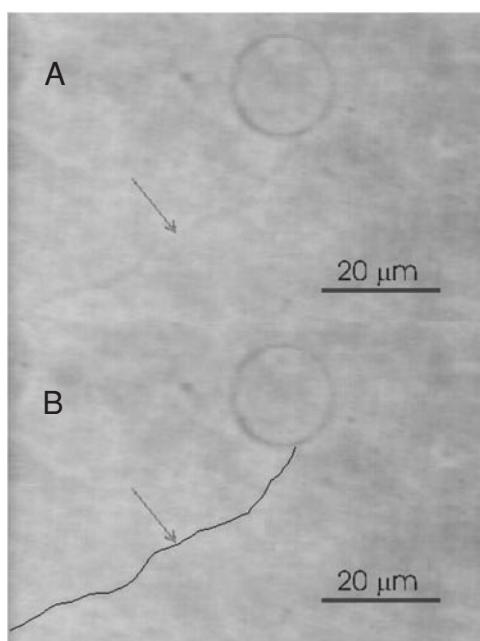


**Figure 4.** (A) A giant phospholipid vesicle (made of POPC in pure water) with a long thin tubular protrusion. The vesicle was observed in the closed chamber made of cover glasses, several hours after preparation. The figure shows the barely visible protrusion, as it is observed in the beginning of the process. (B) A duplicate of the picture with a line drawn to help in locating the protrusion.

experiment it was our aim to find out whether the chirality of the membrane constituents is a pre-requisite factor that is responsible for the stability of the thin tubular structures. The POPC molecules are not chiral; however, chirality of the constituents may develop also due to their association with the ions or molecules from the adjacent solution [11]. As many sugars (including glucose) are chiral, we decided to perform the experiment in pure water. It was found that stable tubular protrusions as well as the essential features of the spontaneous shape transformation that were reported in [13] were also observed in the system composed of nonchiral constituents (see section 1). Figure 4(A) shows a first sight of the vesicle with the protrusion in pure water. The protrusion is barely seen. As the mother sphere is floating in the solution while the protrusion is wobbling, it is difficult to focus on the mother sphere and the protrusion at the same time or even to obtain a sharp picture of the protrusion. The line in figure 4(B) is drawn to help in locating the protrusion.

#### 4. Discussion and conclusion

Starting with a single-constituent energy and following the statistical mechanical derivation of the free energy of the phospholipid bilayer membrane we have shown that the terms of the Helfrich bending energy [30] are recovered. However, an additional term is obtained, corresponding to the deviatoric elasticity. This term emerges from the orientational ordering of the phospholipid molecules in those regions of the membrane where there is large difference between the two principal curvatures such as in nano- and microtubular protrusions. Our results are in accordance with the notion that when the dimensions of materials are reduced to micro- and nanometre size, additional properties should be taken into account in order to explain the observed structures.

The theory presented in this work corresponds to the shapes with very thin tubular protrusions. From the observation by phase contrast (figure 4) we cannot determine the

radius of the protrusion when the two lines corresponding to the edges of the cylinder are blurred. The radius may be much smaller than the width of the shade seen in the picture. Further, the observed slow shape transformation indicates that the protrusion exists before it becomes visible and is therefore even thinner than. The possibility should be considered that the radius of the tubular protrusion immediately after formation is very small—as small as the membrane thickness. Direct evidence for the existence of such tubular structures was only recently reported [13], therefore, such situations were hitherto thought of as practically impossible [25].

Stable tubular structures were described by the tilt difference of the membrane constituents in the two membrane layers [23] or tilt of the membrane constituents and chirality [22]. Chirality may result from chirality of the constituent molecules or from chiral arrangement of nonchiral orientationally ordered constituents. Our experimental results show that stable tubular structures can also be observed in systems composed of nonchiral molecules. Chirality may still be present if the phospholipid molecules were arranged in chiral structures. This possibility remains an unanswered question, however, entropic processes connected to the motion of the phospholipid molecules indicate that chiral arrangement of the molecules is rather improbable. Further, as the temperature of our sample was well above the temperature of the gel to liquid crystal phase transition, it is unlikely that the phospholipid molecules exhibit collective tilt.

It was suggested [25] that the effects of the orientational ordering of the phospholipid molecules were not strong enough to cause instability of the flat bilayer with respect to the tubular structure unless the tube radius is very small, e.g. as small as the membrane thickness. The stability condition used in [25] applies to the local density of the membrane free energy and is subject to no geometrical constraints. On the other hand, in our paper we are describing the shape of a vesicle that is constrained with respect to the area of the membrane, the enclosed volume and the difference between the two leaflet areas. To determine the equilibrium shape we apply the condition that the elastic energy of the whole vesicle should be minimized. However, we perform the variation only amid the shapes that fulfil the constraints regarding  $A$ ,  $V$  and  $\Delta A$ . Such shapes are composed of the mother sphere and a long thin protrusion since they correspond to relatively high differences between the two membrane leaflet areas. In these shapes the deviatoric effect is strong enough to make a choice between the shape with the spherical beads and the shape with the cylinder (figure 3). As the involved energy differences are much larger than  $kT$ , the proposed theory describes the stable shapes composed of the mother sphere and thin tubular protrusion well.

We think that in describing the observed features the relevant constraints should be taken into account. In line with this notion, comparing the theoretical and experimental results Fournier and Galatola found [25] that the geometrical constraints could be the reason why in some cases they did not observe the shapes that were predicted by their theory.

However, it should be noted that we are not considering the formation of the phospholipid vesicles in the alternating electric field and therefore cannot explain why the shapes composed of the mother sphere and thin protrusion emerge. The underlying mechanisms are contained in the constraints regarding the membrane area, enclosed volume and the difference between the two membrane leaflet areas.

The theory and experiment presented in this paper were inspired by the experiments where it was indicated [12] that the phospholipid vesicles obtained in the process of electroformation [28] are connected by thin tubular structures. Later, it was observed [13] that the vesicles, which immediately after the formation appear spherical, transform into flaccid fluctuating vesicles in a process where the remnants of thin interconnecting tubular structures that are attached to the vesicles become thicker and shorter and eventually integrate into the membrane of the mother

vesicle [13]. Therefore, the thin tubular network acts as a reservoir for the membrane area and importantly influences the future shape and dynamics of the globular phospholipid vesicles. Further, this mechanism seems to be common and important also in cells [12, 15, 18].

It follows from the above analysis that the deviatoric contribution to the membrane free energy is considerable only in those regions of the vesicle shape where there is a large absolute value of the difference between the two principal curvatures ( $1/|D|$  of the order of a micrometre or smaller). Elsewhere the deviatoric contribution is negligible. Further, for  $1/|D|$  down to tenths of nanometres, the argument of the Bessel function can be approximated by an expansion  $I_0(x) \simeq 1 + x^2/4$ . Also, the exponential and the logarithmic functions in equation (13) can be expanded up to the linear terms to yield the dimensionless bending energy with renormalized constants

$$f = \frac{1}{4} \left( 1 - \frac{1}{4} \vartheta d_m^2 \right) \int (2h)^2 da + \left( \kappa_G + \frac{1}{4} \vartheta d_m^2 \right) \int c_1 c_2 da. \quad (32)$$

It was taken into account that

$$d^2 = h^2 - c_1 c_2. \quad (33)$$

We have used in our calculations presented in figure 3 and in table 1 the modified Bessel function; however, we have checked the results also by using equation (32) for the shape with the cylindrical protrusion. There was no difference between the results obtained in both ways. Therefore, for the considered tubular shapes the Helfrich energy with renormalized constants can be used. It should however be pointed out that in the shape with the protrusion composed of small spheres connected by infinitesimal necks such renormalization cannot be used, as in the infinitesimal necks the local deviator increases beyond limit. As stated above, the numerical results indicate that there is no contribution of the infinitesimal necks to the free energy. There is also no deviatoric contribution from the spherical parts as the local deviator there is equal to 0. Therefore, in the case of spherical beads the Helfrich free energy with original constants is used

$$f = \frac{1}{4} \int (2h)^2 da + \kappa_G \int c_1 c_2 da. \quad (34)$$

Although the form of the energy is the same in both cases, there is a difference in the energy due to renormalization of the constants in the case of the shape with a cylindrical protrusion. Also, it can be seen that the Gaussian term should also be considered as the Gaussian bending constant is renormalized as well in the case of nonzero deviatoric contribution. For example, if equation (32) is used for a single sphere where  $c_1 = c_2 = 1/r$  and  $r$  is the normalized radius of the sphere, the terms due to renormalization cancel leaving the free energy in the form of equation (34). In other words, if the deviatoric effect is taken into account by the renormalized Helfrich energy, the respective shapes that have the same topology have different Gaussian contributions.

The mechanism of the spontaneous shape transformation that was observed in experiments [13] remains largely obscure. The tubular character of the protrusions may persist even when the protrusions become thicker while more peculiar shapes with undulated protrusions can also be found (figure 5(B)). Also, the timing of the transformation may vary from minutes to hours, as the protrusions are initially of very different lengths (figure 5(A)). In order to understand the mechanisms of the shape transformation in more detail, experiments with controlled environmental conditions should be performed.

If the tubular protrusion becomes thicker in the process of the spontaneous shape transformation the curvature decreases and the deviatoric contribution may become negligible, unless the protrusion develops necks that render minima in the  $f(\Delta a)$  curve [29]. Indeed,

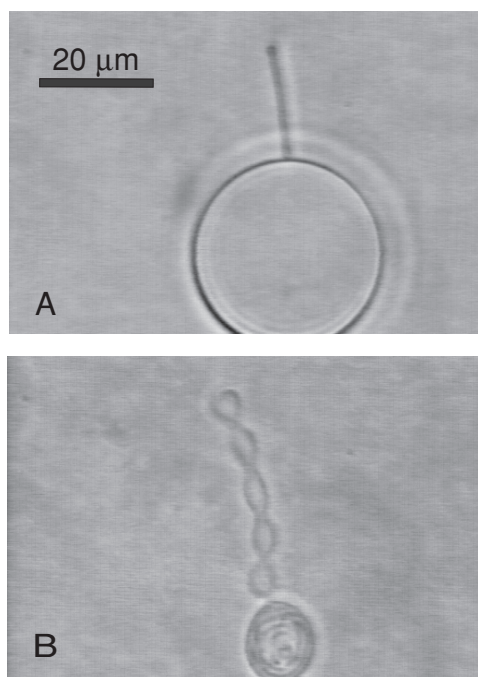


**Figure 5.** Shapes of giant phospholipid vesicles (made of POPC in pure water): a shape with a rather short tubular protrusion (A) and a shape with an undulated protrusion (B). Note the multilamellar structure inside the globular part of shape B. The shape A was observed about 15 min after the vesicles were rinsed into the observation chamber while the shape B was observed several hours later.

oscillations of the neck width with time were observed, indicating increased stability of the necks (not shown). A similar effect—the persistence of the neck connecting a spherical daughter vesicle and a mother vesicle—was observed also in the opening of the neck induced by cooling while the formation of the neck by heating was quick and occurred at higher temperature, indicating hysteresis [36]. The undulations of the protrusion producing the necks could therefore provide a mechanism that would also keep the curvature deviator as high as possible and therefore the membrane free energy as low as possible in the shapes of lower  $\Delta a$ .

If the tube radius were only several nanometres, the thickness of the membrane itself ( $\approx 5$  nm) is comparable to the radius of the protrusion. Besides other effects that may emerge for very thin tubes, the expression for the area difference (equation (21)) should be restated [37] by considering that the membrane thickness is not very small compared to the dimensions of the protrusion. Also, within the presented theory the size and shape of the area occupied by the phospholipid molecule was not taken into account. The generalized bilayer couple model [38] considers that the area per molecule may be different in the two membrane layers, but equal within each layer. This effect is referred to as the relative stretching of the two layers. We have estimated the effect of the relative stretching on the calculated stable shape (results not shown) and found that it is negligible in the region of the long thin protrusions that are the scope of this study.

The deviatoric membrane properties induced by the anisotropic inclusions represent a plausible mechanism for explanation of nonspherical vesicles released from the erythrocyte membrane upon intercalation of some particular species of amphiphiles into the membrane [39, 40, 15]. Peculiar torocyte-shaped endovesicles having a thin plate-like central part and a bulbous toroidal rim were found in erythrocytes incubated with octaethyleneglycoldodecylether (C12E8) [39] and explained by deviatoric properties of the membrane induced by orientational ordering of anisotropic membrane inclusions [40]. Tubular nanoexovesicles were obtained when the erythrocytes were incubated with a dimeric surfactant



[15]. In the dimeric surfactant molecule, the two units (each composed of a headgroup and a tail) are connected by a short spacer, therefore the molecule is highly anisotropic [26]. However, the tubular nanoexovesicles were also obtained when the erythrocytes were incubated with dodecylmaltoside, which is composed of one tail and a large two-unit headgroup [41].

It seems therefore that the anisotropy of the membrane constituent may not only originate in the two-tailed structure, but also in the configuration and shape of the headgroup and its interactions with the surrounding membrane constituents. A possibility should be considered that in the thin phospholipid tubes the configuration of the headgroups may be different from that in almost flat parts. As the interaction constants  $\xi$  and  $\xi^*$  were estimated from the isotropic bending constant  $k_c$  that was determined by considering an almost flat membrane, the estimated values of  $\xi$  and  $\xi^*$  may be considered as a lower bound.

It was already suggested by Fischer [42] that the phospholipid molecules with two hydrocarbon chains are in general anisotropic despite the motion of their segments within the membrane layer. Based on decomposition of the elastic continuum into isotropic and deviatoric bendings, he proposed an expression for the membrane local free energy

$$F = 2B_s \int (H - C_0/2)^2 dA + 2B_a \int (|D| - \theta)^2 dA \quad (35)$$

where  $B_s$  and  $B_a$  are the constants of the isotropic and the deviatoric bending, respectively,  $C_0$  is the spontaneous curvature of the membrane and  $\theta$  is the spontaneous warp. The spontaneous warp should originate from the anisotropy of the constituent molecules. However, he then claimed that spontaneous warp is negligible for one component phospholipid membrane due to the fact that the membrane of such a vesicle, as observed in experiments, is locally flat. He argued that for a nonzero spontaneous warp the membrane would be corrugated. Our results may contribute to the clarification of the issues raised by Fischer [42]. Our experimental results presenting shapes with tubular protrusions show that the membrane is not flat. However, the bilayer is organized rather in a few longer protrusions than in numerous shorter folds. This seems to be energetically more favourable taking into account that the beginning and the end of the protrusion have high isotropic bending energy. It must also be considered that the shape of the vesicle is subject to constraints regarding the membrane area, enclosed volume and the numbers of molecules constituting both layers. The shape with folds would have considerably lower relative volume and higher difference between the two membrane layer areas than the smooth shape of roughly equal appearance, therefore, the two shapes would be rather far apart in the phase diagram of the possible shapes. Shifting from one point to the other may involve processes required to overcome the energetic barrier(s), i.e. due to isotropic bending energy [29]. Further, it is shown theoretically that the deviatoric effect is usually not uniformly distributed over the area of the vesicle so that in this respect the description by spontaneous warp (equation (35)) is oversimplified. Nevertheless, our results support the general ideas of deviatoric elasticity proposed by Fischer.

Our results indicate that the description of the isotropic intrinsic effective shape of membrane constituents [43] should be upgraded by considering a possible anisotropy of the constituents. We propose that the effective intrinsic shape is given by the two constants  $H_m$  and  $D_m$ .

In the phospholipid bilayer membrane it was considered that there is hexatic ordering of the constituent molecules. This means that there is orientational but no positional ordering. Further, the orientational ordering was subject to entropic processes and therefore not uniform within the regions of the uniform curvature field. However, the principle of deviatoric elasticity can also be applied to systems with higher degrees of ordering such as inorganic micro- and nanotubes.

To conclude, deviatoric elasticity is a simple mechanism that provides an explanation of stable strongly anisotropic structures attached to the mother sphere of a phospholipid vesicle.

## Acknowledgment

We are grateful to P Peterlin for help with electronic preparation of the manuscript.

## References

- [1] Iijima S 1991 *Nature* **354** 56
- Srolovitz D J, Safran S A, Homyonfer M and Tenne R 1995 *Phys. Rev. Lett.* **74** 1779
- Yakobson B I, Brabec C J and Bernholc J 1996 *Phys. Rev. Lett.* **76** 2511
- [2] Marx W, Wanitschek M and Schier H 1999 *Condensed Matter News* **7** 3
- [3] Chopra N G, Luyken R J, Cherrey K, Crespi V H, Cohen M L, Louie S G and Zettl A 1995 *Science* **269** 966
- Rao A M, Richter E, Bandow S, Chase B, Eklund P C, Williams K A, Fang S, Subbaswamy K R, Menon M, Thess A, Smalley R E, Dresselhaus G and Dresselhaus M S 1997 *Science* **275** 187
- [4] Remškar M, Škraba Z, Regula M, Ballif C, Sanjines R and Levy F 1998 *Adv. Mater.* **10** 2
- Remškar M, Škraba Z, Cleton F, Sanjines R and Levy F 1998 *Surf. Rev. Lett.* **5** 423
- Tans S J, Verschueren R M and Dekker C 1998 *Nature* **393** 49
- [5] Nakamura H and Matsui Y 1995 *J. Am. Chem. Soc.* **117** 2651
- Hoyer P 1996 *Langmuir* **12** 141
- [6] Han W Q, Fan S S, Li Q Q and Hu Y D 1997 *Science* **277** 1287
- [7] Guo L, Wu Z, Liu T, Wang W and Zhu H 2000 *Chem. Phys. Lett.* **318** 49
- [8] Seifert G, Terrones H, Terrones M and Frauenheim T 2000 *Solid State Commun.* **15** 635
- [9] Schnur J M 1993 *Science* **262** 1669
- [10] Chiruvolu S, Warriner H E, Naranjo E, Kraiser K, Idziak S H J, Radler J, Plano R J, Zasadzinsky J A and Safinya C R 1994 *Science* **266** 1222
- Safinya C R 1997 *Colloids Surf. A* **128** 183
- Težak D, Punčec S and Martins M 1997 *Liq. Cryst.* **23** 17
- Shahidzadeh N, Bonn D, Aguerre-Chariol O and Meunier J 1998 *Phys. Rev. Lett.* **81** 4268
- Shahidzadeh N, Bonn D, Aguerre-Chariol O and Meunier J 1999 *Colloids Surf. A* **147** 375
- [11] Oda R, Huc I, Schmutz M, Candau S J and MacKintosh F C 1999 *Nature* **399** 566
- [12] Mathivet L, Cribier S and Devaux P F 1996 *Biophys. J.* **70** 1112
- [13] Kralj-Iglič V, Gomišček G, Majhenc J, Arrigler V and Svetina S 2001 *Colloids Surf. A* **181** 315
- [14] Lutz H U, Lomant A J, McMillan P and Wehrli E 1977 *J. Cell Biol.* **74** 389
- Coakley W T, Bater A J and Deley J O T 1978 *Biochim. Biophys. Acta* **512** 318
- [15] Kralj-Iglič V, Iglič A, Hägerstrand H and Peterlin P 2000 *Phys. Rev. E* **61** 4230
- [16] Kralj-Iglič V, Iglič A, Hägerstrand H and Bobrowska-Hägerstrand M 2001 *Colloids Surf. A* **179** 57
- [17] Ochs S, Pourmand R, Jersild R A Jr and Friedman R N 1997 *Prog. Neurobiol.* **52** 391
- [18] Kralj-Iglič V, Batista U, Hägerstrand H, Iglič A, Majhenc J and Sok M 1998 *Radiol. Oncol.* **32** 119
- [19] Nelson D, Piran T and Weinberg S (ed) 1989 *Statistical Mechanics of Membranes and Surfaces* (Singapore: World Scientific)
- Lasic D D and Barenholz Y (ed) 1996 *Handbook of Nonmedical Applications of Liposomes* (Boca Raton, FL: CRC Press)
- [20] de Gennes P G 1987 *C. R. Acad. Sci. Paris* **304** 259
- [21] Helfrich W and Prost J 1988 *Phys. Rev. A* **38** 3065
- [22] Selinger J V, MacKintosh F C and Schnur J M 1996 *Phys. Rev. E* **53** 3804
- [23] Seifert U, Schillcock J and Nelson P 1996 *Phys. Rev. Lett.* **77** 5237
- [24] Boulbitch A A 1997 *Phys. Rev. E* **56** 3395
- [25] Fournier J B and Galatola P 1997 *J. Physique* **7** 1509
- [26] Fournier J B 1996 *Phys. Rev. Lett.* **76** 4436
- [27] New R R C 1990 *Liposomes, a Practical Approach* (Oxford: Oxford University Press) p 8
- [28] Angelova M I, Soleau S, Meleard Ph, Faucon J F and Bothorel P 1992 *Prog. Colloid Polym. Sci.* **89** 127
- [29] Kralj-Iglič V, Heinrich V, Svetina S and Žekš B 1999 *Eur. Phys. J. B* **10** 5
- [30] Helfrich W 1973 *Z. Naturforsch.* **28c** 693
- [31] Duwe H P, Käs J and Sackmann E 1990 *J. Physique* **51** 945



- [32] Seifert U 1997 *Adv. Phys.* **46** 13
- [33] Cevc G and Marsh D 1987 *Phospholipid Bilayers* (New York: Wiley-Interscience)
- [34] Sheetz M P and Singer S J 1974 *Proc. Natl. Acad. Sci. USA* **72** 4457  
Evans E A 1974 *Biophys. J.* **14** 923  
Helfrich W 1974 *Z. Naturforsch.* **29c** 510
- [35] Svetina S and Žekš B 1985 *Biomed. Biochim. Acta* **44** 979
- [36] Käs J and Sackmann E 1991 *Biophys. J.* **60** 825
- [37] Szleifer I, Kramer D, Ben-Shaul A, Gelbart W M and Safran S A 1990 *J. Chem. Phys.* **92** 6800
- [38] Evans E A 1980 *Biophys. J.* **30** 265  
Miao L, Seifert U, Wortis M and Döbereiner H G 1994 *Phys. Rev. E* **49** 5389  
Svetina S, Iglič A and Žekš B 1994 *Ann. N.Y. Acad. Sci.* **710** 179
- [39] Bobrowska-Hägerstrand M, Kralj-Iglič V, Iglič A, Bialkowska K, Isomaa B and Hägerstrand H 1999 *Biophys. J.* **77** 3356
- [40] Iglič A, Kralj-Iglič V, Božič B, Bobrowska-Hägerstrand M and Hägerstrand H 2000 *Bioelectrochemistry* **52** 203
- [41] Hägerstrand H and Isomaa B 1992 *Biochim. Biophys. Acta* **1109** 117
- [42] Fischer T 1992 *J. Physique* **2** 337  
Fischer T 1993 *J. Physique* **3** 1795
- [43] Israelachvili J 1992 *Intermolecular and Surface Forces* 2nd edn (London: Academic) p 381